ACS APPLIED POLYMER MATERIALS

pubs.acs.org/acsapm

Article

Design of Highly Thermally Conductive Hexagonal Boron Nitride-Reinforced PEEK Composites with Tailored Heat Conduction Through-Plane and Rheological Behaviors by a Scalable Extrusion

Saher Gul, Selin Arican, Murat Cansever, Bertan Beylergil, Mehmet Yildiz, and Burcu Saner Okan*

Cite This: *ACS Appl. Polym. Mater.* 2023, 5, 329−341

Read Online

ACCESS | Metrics & More | Article Recommendations | Supporting Information

ABSTRACT: The challenge of developing highly thermally conductive polymeric composites to meet the growing thermal management demands has recently attracted a lot of attention. To achieve a through-plane thermal conductivity higher than 2 W/mK, a high filler concentration within the poly(ether ether ketone) (PEEK) matrix is required, thus adding to the complexity of polymer processing. In this study, an optimized twin-screw extrusion melt-compounding technique was developed by tuning the melt flow of unfilled PEEK, feeding zones, and process cycles for dispersion of hexagonal boron nitride (h-BN) in the PEEK polymer. The prepared composites demonstrated exceptionally high in-plane and through-plane thermal conductivity of 12.451 and 2.337 W/mK, respectively, at 60 wt % h-BN loading. This improvement of thermal conduction in both directions can be attributed to two factors: (1) formation of through-thickness surface contacts between h-BN particles due to shear-driven exfoliation during compounding stage and (2) high degree of alignment of h-BN platelets achieved during molding stage. The calorimetric and thermogravimetric analyses indicated that the prepared composites possess enhanced crystallinity compared to unfilled PEEK and are thermally stable in elevated temperature ranges. The rheological characterization exhibited a progressive increase in viscosity and shear-thinning behavior of composite melts proportional to the h-BN concentration. Using the temperature and time-dependent rheological results, viscosity buildup profiles were constructed to outline allowable melt viscosity ranges for each composite composition. These profiles can be utilized to tailor the residence time of a composite melt by varying the filler concentration and process temperature during advanced manufacturing processes such as extrusion-based additive manufacturing and powder bed fusion. Hence, we provide a facile and industrially scalable method for development of h-BN-filled PEEK composites with high thermal dissipation characteristics aimed for thermal management in various harsh environment applications.

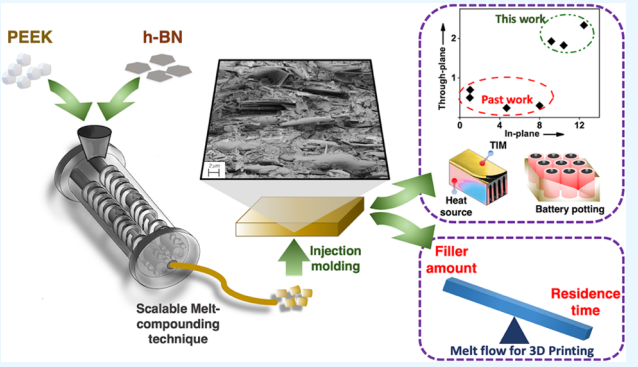

KEYWORDS: *thermal conductivity, rheology, melt-compounding, through-plane thermal conductivity, poly(ether ether ketone), PEEK, hexagonal boron nitride, polymer composites*

1. INTRODUCTION

Efficient dissipation of heat and control of any sudden temperature changes in high-density electronic devices remain major technological challenges in the automotive and aerospace industries. Since volume allotments in these industries have shrunk rapidly to ensure portability, the development of compact and lightweight materials with enhanced thermal conductivity has become critical for the prevention of local heat hot spots and thermal fatigue.[1,2] Although poly(ether ether ketone) (PEEK) offers extraordinary performance in terms of high-temperature tolerance, chemical resistance, and dimensional stability,[3,4] it cannot satisfy the requirements of high heat removal rates because of its extremely low intrinsic thermal conductivity. To date, there have been numerous studies indicating that the thermal conductivity (T.C) of PEEK can be improved by introduction of metallic or carbon-based additives in the polymer.[5−7] For instance, Hwang et al. improved the thermal conductivity of PEEK 2-fold (~0.44 W/mK) by solution mixing of 1 wt % graphene oxide filler in the matrix.[6] Similarly, Liu et al. produced a hierarchical structure using graphene and carbon fibers as fillers in the PEEK polymer through a two-step sonication and ball milling technique, increasing the thermal conductivity of PEEK/carbon fiber laminates by 53.7% due to continuously

Received: September 1, 2022
Accepted: November 16, 2022
Published: December 1, 2022

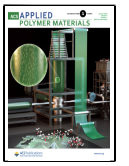

connected network of graphene sheets in the matrix at a graphene loading of 0.7 wt %.[7] Although these kinds of carbon fillers can improve the thermal conductivity of host polymers, they also increase the electrical conductivity of the manufactured composites at the same time, likely to cause current leakage and short circuit problems when used as thermal interface materials (TIMs) for electronic packaging.[8,9] Therefore, in areas requiring thermal conduction and electrical insulation, instead of metallic or carbon-based additives, ceramic materials have been widely preferred as thermally conductive agents.[10−13]

Among such ceramic fillers, hexagonal boron nitride (h-BN) has captured widespread interest due to its high intrinsic thermal conductivity, excellent electrical insulation, low dielectric constant, and high dielectric breakdown strength.[14,15] The experimentally measured thermal conductivity of the basal plane of h-BN has been reported to be as high as 390 W/mK,[16] making it a promising candidate for the development of thermally conductive polymeric materials. In one of the recent works, Xie et al. evaluated the thermal conductivity of polyvinyl alcohol/hydroxylated-h-BN composites produced via a solution blending method, reporting an in-plane T.C of 3.92 W/mK at 10 wt % filler loading due to homogeneous dispersion and high degree of filler orientation.[17] In another study, Su et al. fabricated a composite structure using spheroidized h-BN fillers in the polyurethane matrix, attaining an impressive in-plane thermal conductivity of 7.2 W/mK due to three-dimensional phonon transfer with 40 wt % filler loading.[18] Overall, the generation of efficient heat conduction pathways in directions parallel and perpendicular to the heat conduction is greatly influenced by the dispersibility and orientation of the h-BN platelets within the polymer matrix. Although, various works have improved the in-plane thermal conductivity of engineering plastics, the enhancement of through-plane T.C, especially in high-temperature thermoplastics, still remains a challenge due to agglomeration and defect formation in h-BN fillers during composite processing stages.[19] In other words, the dispersion of bulk h-BN is difficult due to strong lip−lip interactions between neighboring h-BN layers, which leads to a higher exfoliation energy of h-BN.[20]

To increase the degree of exfoliation and interfacial surface area of h-BN particles within the matrix, the method used for the integration of h-BN in the polymer carries great importance.[21,22] Although solution mixing has been frequently utilized for this purpose, it poses limitations during the processing of engineering polymers due to the use of highly corrosive acids for dispersion of h-BN,[23,24] making it less suitable for PEEK due to the polymer's chemically inert nature in common solvents. Therefore, for high-performance thermoplastics such as PEEK, filler integration *via* melt-blending techniques is a more appropriate method since it is capable of providing physical exfoliation of the h-BN sheets through the polymer chains upon application of high shear/compression forces without requiring a solvent.[25−27] An important factor to consider during melt-blending via twin-screw extrusion processes is the screw design.[28,29] For instance, Muller et al. have shown that the screw profile has a pivotal effect on the dispersion and distribution of a filler with a layered morphology within the polymer matrix and suggested that side feeding the filler into an already molten polymer can facilitate better dispersion, thus resulting in better mechanical performance.[29]

Researchers have regularly observed that the random spatial distribution of h-BN particles in a melt-blended premix is heavily disturbed during the part manufacturing steps, and due to preferential alignment of the fillers in the matrix, the out-of-plane T.C remains small compared with the in-plane direction.[30,31] In a recent investigation by Liu et al., melt blended PEEK/h-BN specimens exhibited a through-plane conductivity of 0.5 W/mK at 30 wt % filler loading, which was very low compared to the in-plane value because h-BN sheets had made contacts primarily in the in-plane direction during molding.[32] Similar results were reported by Wang et al., in which the perfect in-plane arrangement of h-BN nanosheets during composite fabrication caused an extreme anisotropy between the thermal conductivity values. At a loading of 13.4 vol %, the through-plane T.C was reported to be 0.3 W/mK in contrast to 8 W/mK in the in-plane direction.[31]

Achieving a simultaneous enhancement in the in-plane and through-plane thermal conductivity of the h-BN-filled composites is quite challenging due to the requirement of a very high filler concentration, which severely affects the processability of the thermoplastic polymers during melt-mixing and composite manufacturing steps.[33] Through-plane and in-plane thermal conductivity enhancement of PEEK polymer using h-BN fillers to obtain a well-rounded thermally conductive material has been largely overlooked and the available studies are either related to functionalized/modified h-BN particles, use a low filler amount, and/or deal exclusively with in-plane conductivity enhancement.[34,35] Therefore, there is a need for a scalable filler integration process, which not only is capable of forming continuous three-dimensional heat conduction networks within the h-BN-filled polymer composites but also can accommodate a very high filler content without compromising the filler dispersibility.

Herein, we report a through-plane thermal conductivity value exceeding 2 W/mK in PEEK-based h-BN composites developed *via* a scalable twin-screw extrusion approach for the dispersion of h-BN fillers. By tailoring the raw material feeding zones, feeding amount, melt flow of PEEK, and process cycles, micron-sized h-BN is uniformly integrated in a range of 5−60 wt % in the PEEK polymer matrix to achieve a well-connected network of h-BN sheets without degradation at high-temperature processing conditions. As a result, we obtained the highest in-plane and through-plane thermal conductivity values of the PEEK/h-BN composites reported thus far in the literature. To understand the effect of the degree of exfoliation and spatial orientation of h-BN platelets on the heat transfer in PEEK/h-BN composites, a comprehensive physical and thermoanalytical characterization of the prepared specimens was executed. Furthermore, this paper discusses the influence of polymer/filler phase interactions and filler aggregation in governing the changes in the mechanical properties of the PEEK/h-BN composites. Rheological characterization as a function of frequency, temperature, and time was also carried out to establish a link between the filler−matrix interface, filler alignment, and flow characteristics of the PEEK/h-BN composites, and a framework is suggested for design of an ideal feedstock composition through the correlation of rheological properties of composites to the process parameters of advanced additive manufacturing methods.

2. EXPERIMENTAL SECTION

2.1. Materials. Unfilled PEEK polymer in pellet form under the trade name of Tecopeek PK40 NL pellets was provided by Eurotec

https://doi.org/10.1021/acsapm.2c01534
ACS Appl. Polym. Mater. 2023, 5, 329−341

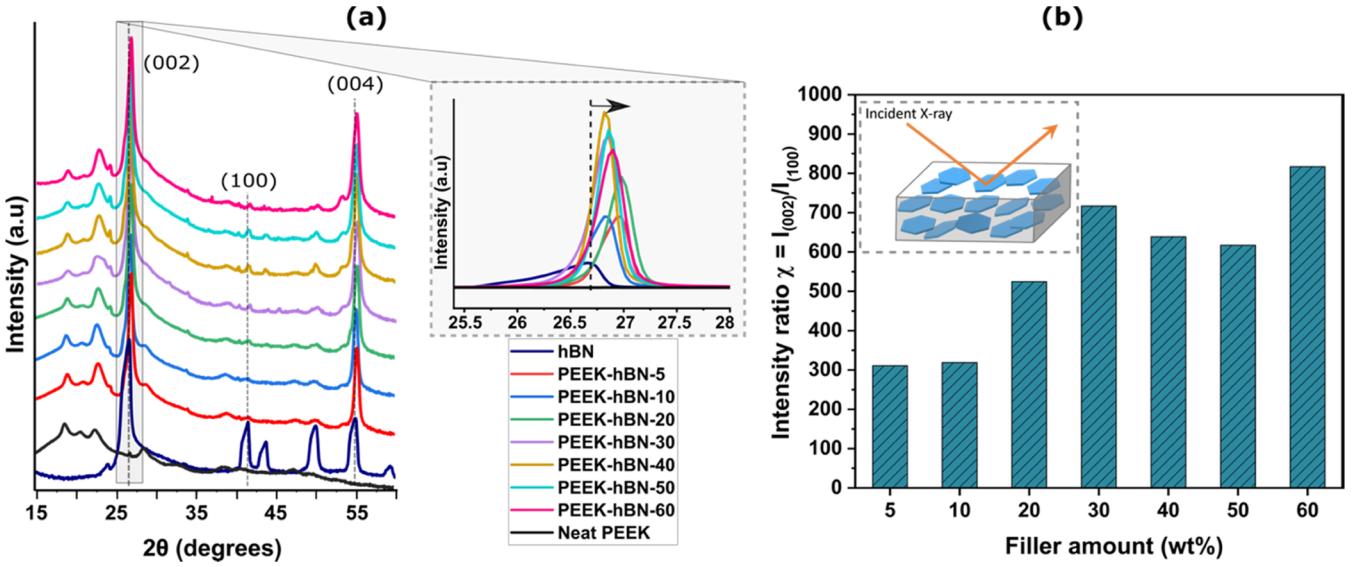

Figure 1. (a) XRD patterns of PEEK/h-BN composites and starting materials with the inset showing enlarged 2θ range from 25.5° to 28° and (b) intensity ratio of the (002) and (100) crystallographic planes of the PEEK/h-BN composites as a function of the h-BN concentration with the inset depicting the sample orientation with respect to incident X-ray during XRD analysis.

(Turkey). PEEK has a density of 1.30 g/cm^3 and melt flow index (MFI) of 92.08 g/10 min at 380 °C/5 kg, as reported by the material supplier. Hexagonal boron nitride (h-BN) powder with a median particle size of 25−30 μm was purchased from Henze (Germany) with product code HeBoFill 490 and used as received without any surface modification.

2.2. Fabrication of PEEK/h-BN Compounds by Twin-Screw Extrusion. For manufacturing of the PEEK/h-BN composites, melt-compounding was carried out using a co-rotating twin-screw extruder ZSK26 MC of Coperion, GmbH (Stuttgart, Germany) with diameter = 26 mm and L/D = 40. The h-BN filler in various amounts from 5−60 wt % was compounded with the PEEK granules to achieve the target thermal conductivity values. Since screw configuration plays an essential role in the feeding and distribution of the h-BN additive, various screw configurations were tried during the compounding process by optimizing the number of kneading/mixing and reverse elements. After selecting suitable process parameters, PEEK/h-BN compounds were extruded at barrel temperatures between 400−450 °C and pelletized. Before extrusion, PEEK granules and the h-BN powder were vacuum-dried at 150 °C for 4−6 h.

For further characterization, the compounded pellets were injection-molded into test specimens with the following molding parameters: feed throat temperature = 80−100°C, processing temperature = 390−450 °C, mold temperature = 200−250 °C, and hold pressure = 200−250 MPa. Names of the prepared composite samples are expressed as PEEK-hBN-X, where X stands for the concentration (wt %) of h-BN (Table S1).

2.3. Characterization. X-ray diffraction (XRD) analysis was performed using a D2 Phaser diffractometer (Bruker) equipped with a Cu Kα source to investigate the crystalline structure of injection-molded samples. For morphological investigation, mechanical test samples were fractured and sputter-coated with a thin layer of gold; later, the fracture surface was analyzed using Leo Supra 35V field emission scanning electron microscope (SEM). Furthermore, thermal analysis of the polymer compounds was conducted using differential scanning calorimetry (DSC) on a DSC 3+ module (Mettler Toledo). First, the PEEK/h-BN samples were heated to 450 °C at a rate of 10 °C/min to remove the thermal history, then cooled down to room temperature at a rate of −10 °C/min, and the samples were heated again to 450 °C at a rate of 10 °C/min. Quantification of the thermal stability of composite samples in a nitrogen atmosphere was done using thermal gravimetric analysis (TGA) with a TGA/DSC 3+ module (Mettler Toledo) between 25 and 1000 °C. In-plane and through-plane thermal conductivities were measured according to the ISO 22007-4 standard. The measurement technique is a transient laser flash method, whereby thermal conductivity is calculated using the following equation

$$\kappa = \alpha . \rho . C_p \quad (1)$$

where κ is the thermal conductivity, α is the thermal diffusivity calculated from specimen thickness and time needed for the temperature rise to reach a percentage of its maximum value, ρ is the density, and C_p is the specific heat.

The rotational and oscillatory rheological data were measured using an MCR 702 Twin Driver rheometer (Anton-Paar, Austria) fitted with 25 mm disposable parallel plate geometry to obtain the frequency, temperature, and time-dependent viscoelastic properties. The frequency sweep tests were conducted from 0.06 to 628.32 rad/sec at 380 °C to observe the variation of rheological properties with the change in frequency. To remain within the viscoelastic limit, for samples up to 30 wt % h-BN, the shear strain was kept at 1%, while for higher loadings, a shear strain of 0.1% was utilized to obtain consistent frequency sweep results. For temperature-dependent measurements, the temperature range was 350−440 °C, while the shear strain and frequency during the tests were kept constant at 10 Hz and 1%, respectively. Moreover, time-sweep tests were conducted for 45 min at a low frequency (1 Hz) and low shear strain (1%) at 380 °C. For all tests, the gap between the parallel plates was kept between 1.8 and 2.5 mm.

Tensile tests on composite specimens were performed by a universal test machine (UTM) at a constant crosshead speed of 1 mm/min as per the ISO 527 standard. Furthermore, flexural properties were measured using a three-point bending test according to the ISO 178 test standard with a constant crosshead speed of 2 mm/min, and Izod impact tests were conducted according to the ISO 180 standard at 25 °C.

3. RESULTS AND DISCUSSION

3.1. Effect of h-BN Concentration on the Crystalline and Thermal properties of PEEK/h-BN Compounds. Alignment of the h-BN particles formed within the polymer matrix during filler integration stages and the subsequent specimen manufacturing steps greatly influences the in-plane and through-plane thermal conductivities of the prepared composites. Therefore, to understand the state of h-BN dispersion and filler orientation within the composite samples,

https://doi.org/10.1021/acsapm.2c01534
ACS Appl. Polym. Mater. 2023, 5, 329−341

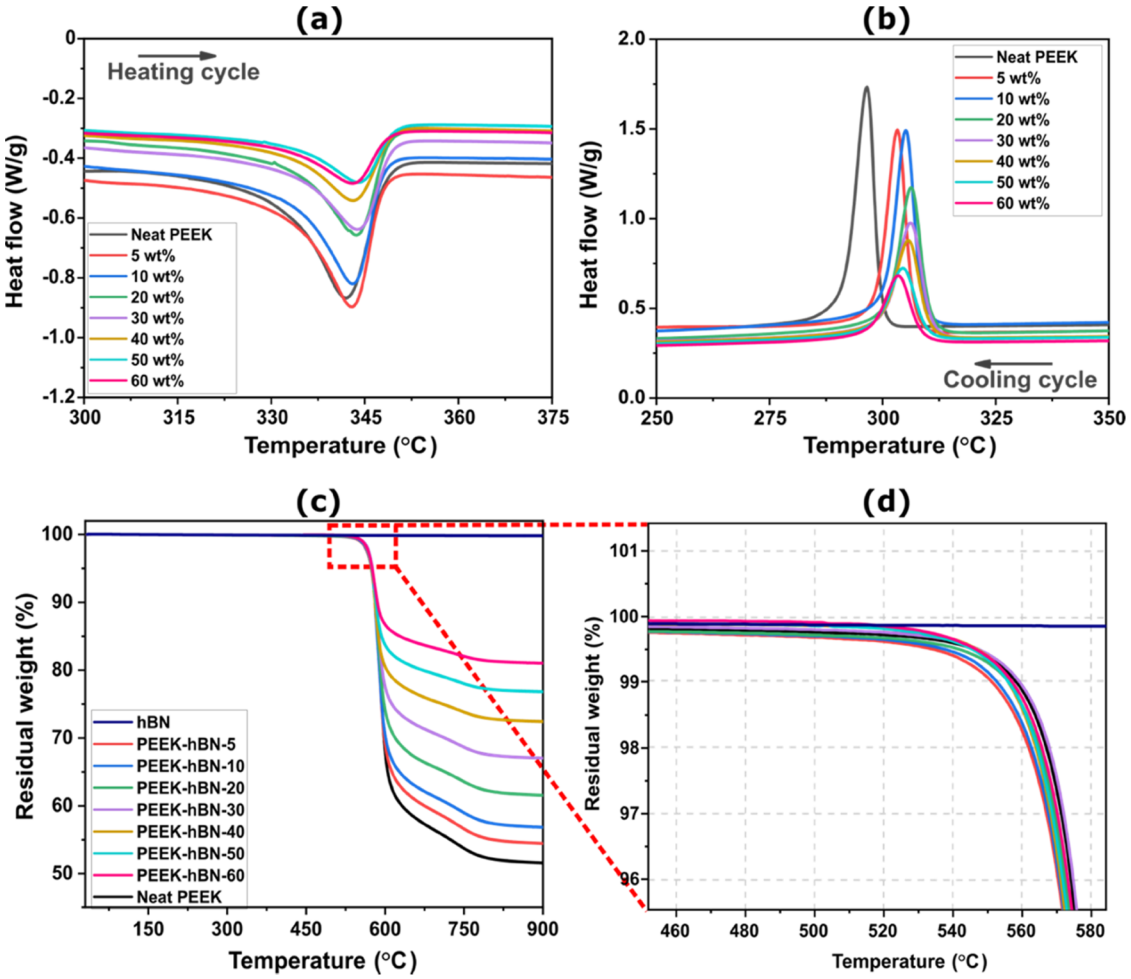

Figure 2. Thermal phase transitions and thermal stability of the PEEK/h-BN composites. DSC thermographs of the composites during the (a) heating cycle showing the melting peak and (b) cooling cycle showing the crystallization peak. TGA thermograms of (c) starting materials and composites and (d) enlarged view of (c) showing the onset of decomposition in a nitrogen atmosphere.

X-ray diffraction analysis is performed on the injection-molded samples. Figure 1a shows the XRD patterns of PEEK/h-BN composites and the starting bulk materials (PEEK polymer and h-BN powder). For the semicrystalline PEEK polymer, the typical characteristic peaks with 2θ values of 18.7, 20.7, 22.45, and 28.59° corresponding to the (110), (111), (200), and (211) planes can be observed.[36,37] Whereas, for the bulk h-BN specimen, the principal reflection is located at 2θ = 26.6° due to the (002) crystallographic plane of h-BN platelets, and the weaker peaks in the patterns are due to the (100), (101), (102), and (004) planes at 2θ = 41.55, 43.85, 50.09, and 54.91°, respectively[38,39] (Figure S1). As depicted in Figure 1a, the addition of h-BN platelets into PEEK results in the appearance of two prominent peaks relating to the (002) and (004) planes in all of the composite specimens, resulting mainly due to horizontally orientated h-BN particles within the matrix. Moreover, the drastic drop in the peak intensity I of the (100) plane for the composite specimens hints toward a lower amount of through-plane aligned h-BNs compared to the in-plane oriented particles.[40] This intensity reduction of the (100) plane suggests an enhanced degree of exfoliation achieved during the melt-compounding process since the high shearing force is able to efficiently overcome the van der Waals forces present between the h-BN flakes, thus separating them.

For a quantitative comparison, a parameter χ is defined such that $\chi = \frac{I_{002}}{I_{100}}$, where I_{002} is the peak intensity of the (002) crystallographic plane and I_{100} is the peak intensity of the (100) plane, to provide additional information about the alignment condition of h-BN platelets within the polymer matrix.[41,42] Figure 1b shows the variation of the intensity ratio χ with the h-BN concentration in the PEEK matrix. For the bulk h-BN, χ is the lowest since the specimen is in a loose powder form and particles are randomly positioned (Table S2). However, after integrating the h-BN particles in the PEEK matrix, intensity ratio rises sharply for the composite specimens as the incident X-ray goes through more (002) horizontal lattice planes compared to the (100) planes. In general, the higher the loading amount of the filler, the higher the intensity ratio. For example, it is found that χ of PEEK composites with 60 wt % h-BN filler is at least 2.6 times larger than that of PEEK-hBN-5. The increase in χ is associated to the high degree of orientation of the horizontal lattice planes of h-BN particles parallel to the flow direction during injection-molding such that the spatial orientation of the h-BN filler is no longer random. Highly orientated filler platelets also have an essential effect on the enhancement of in-plane thermal conductivity of the PEEK/h-BN composites, as elaborated further in upcoming sections.

https://doi.org/10.1021/acsapm.2c01534
ACS Appl. Polym. Mater. 2023, 5, 329−341

The XRD parameters of the composite specimens have been summarized in Table S2. It is observed that for the composite samples, the corresponding 2θ values for the (002), (100), and (004) planes remain between 26.71 and 26.97, 41.41 and 41.65°, and 55.03 and 55.27°, respectively. The XRD patterns of the composites show a shift toward higher 2θ values for the (002) plane compared to the bulk h-BN powder, signaling a decrease in the lattice parameters of the filler.[43] A similar shift is observed for the (004) plane, where the (004) plane is parallel to the (002) plane. In conclusion, XRD analysis of the composite specimens shows that the crystalline structure formed on the addition of h-BN platelets in the PEEK matrix is stable and no phase change in the material is observed on increasing the filler amount from 5 to 60 wt %. Furthermore, the degree of orientation of h-BN particles within the PEEK matrix is highly dependent on two factors: (i) the amount of h-BN fillers and (ii) preferential orientation of h-BN platelets parallel to the direction of molding during sample manufacturing.

The thermal analysis of samples is performed using DSC and TGA characterizations for the evaluation of structural transitions and stability of the prepared composites in response to the change in temperature. The effect of filler amounts on the melting and crystallization behaviors of the prepared composites is investigated using nonisothermal DSC measurements. From the recorded melting and crystallization patterns, the thermal parameters such as melting temperature (T_m), melting enthalpy (H_m), crystallization onset temperature (T_c), glass transition temperature (T_g), and degree of crystallization (X_c) were obtained (Table S3). For calculation of the degree of crystallization, the peak enthalpies of the composite specimens were normalized to the corresponding weight fraction of the PEEK polymer (WF_{PEEK}) according to the following formula[44]

$$X_c = \frac{H_m}{H_{PEEK} \times WF_{PEEK}} \times 100 \quad (2)$$

where H_{PEEK} is 130 J/g, the theoretical value of enthalpy for 100% crystalline PEEK polymers.[45]

Figure 2a,b show the heating endotherms and crystallization exotherms for the PEEK/h-BN composites obtained during the second heating and the first cooling cycles, respectively. The endothermic peak corresponding to the melting temperature (T_m) of the unfilled PEEK polymer is located at 342.1 °C. When compared to the pure PEEK, all composite specimens exhibit a slight increase in T_m; for instance, at a 50 wt % filler content, an increase of 1.8 °C in the melting temperature is recorded, while the presence of h-BN particles has hardly any effect on the glass transition temperature of the composites. On the other hand, melt crystallization traces of the composites exhibit a strong correlation with the weight fraction of the h-BN particles. Generally, the peak temperature obtained during the cooling cycle refers to the moment at which the crystallization rate reaches it maximum value.[46] It can be seen in Figure 2b that the peak crystallization temperature values of the prepared composites are higher than that of the pure PEEK. This effect could be explained in terms of the nucleation effect of h-BN particles, which reduces the nucleation energy and increases the crystallization rate of the composite material, thus favoring the early onset of crystallization within the PEEK matrix.[47] The resultant heterogeneous nucleation also renders an improvement in the degree of crystallinity (X_c) of the composites, and in the prepared PEEK/h-BN specimens, X_c increases when the filler amount is increased. As PEEK is a semicrystalline polymer, its degree of crystallinity within the composite specimens can influence the degree of stiffness and heat resistance of the manufactured parts; thus, a higher X_c is generally favored. Table S3 shows that the calculated X_c reaches a maximum value of 40.92% when the filler loading is 60 wt %, compared to 36.23% for the unfilled PEEK sample. The increased degree of crystallinity combined with the hindrance in polymer chain movement due to the characteristic platelet-shaped geometry of h-BN particles improved the melting temperature of the composite samples. So, all of these results seem to suggest that h-BN addition into the PEEK matrix increases the crystallization rate in the composite specimens. At the same time, the glass transition temperature and melting temperature of the PEEK matrix remain largely unaffected.

For a comprehensive thermal analysis, DSC studies were complemented with thermogravimetric analysis (TGA) to evaluate the thermal stability and decomposition behavior of the prepared composites. Figure 2c,d exhibit the TGA curves of neat PEEK and its composites in a nitrogen atmosphere, and detailed data are presented in Table 1.

Table 1. Thermal Stability of PEEK/h-BN Composites in Terms of Weight Loss Percentage at Various Temperatures

	weight loss (%)		
specimen	500 °C	600 °C	900 °C
unfilled PEEK	0.03	32.49	48.42
PEEK-hBN-5	0.31	31.08	45.55
PEEK-hBN-10	0.30	29.55	43.16
PEEK-hBN-20	0.29	25.95	38.45
PEEK-h-BN-30	0.20	22.46	32.97
PEEK-h-BN-40	1.14	19.48	27.58
PEEK-hBN-50	0.14	16.27	23.17
PEEK-hBN-60	0.10	13.28	18.97

The unfilled PEEK polymer undergoes a typical two-step thermal degradation process, whereby first decomposition starting at 575 °C is attributed to the random chain scission of the ether and ketone bonds, while the second decomposition phase occurs due to cracking and dehydrogenation of the cross-linked residue produced in the first stage.[48] A quick and substantial weight loss of nearly 32.49% occurs in the PEEK matrix on reaching 600 °C, followed by slower volatilization of the residue with only 48.42% of the sample left at 900 °C. The addition of the h-BN filler does not have any substantial effect on the thermal degradation onset temperature, and the degradation behavior at temperatures below 600 °C is largely controlled by the PEEK polymer chains and not the filler. However, at elevated temperatures such as 600 and 900 °C, the presence of h-BN particles continues to inhibit the decomposition of composite specimens. For example, with the filler content of 60 wt %, the residue yield at 600 °C is 86.72%, which is nearly 1.3 times higher compared to the unfilled PEEK. The improved thermal stability is due to the strong shielding effect of the h-BN particles, which efficiently delays the escape of the degradation product of the PEEK polymer.[49] Thus, the TGA analysis confirms that the prepared composites can withstand extreme service temperatures without widespread combustion or thermal degradation, and the excellent high-temperature performance of the PEEK polymer is not degraded upon the addition of h-BN particles.

https://doi.org/10.1021/acsapm.2c01534
ACS Appl. Polym. Mater. 2023, 5, 329−341

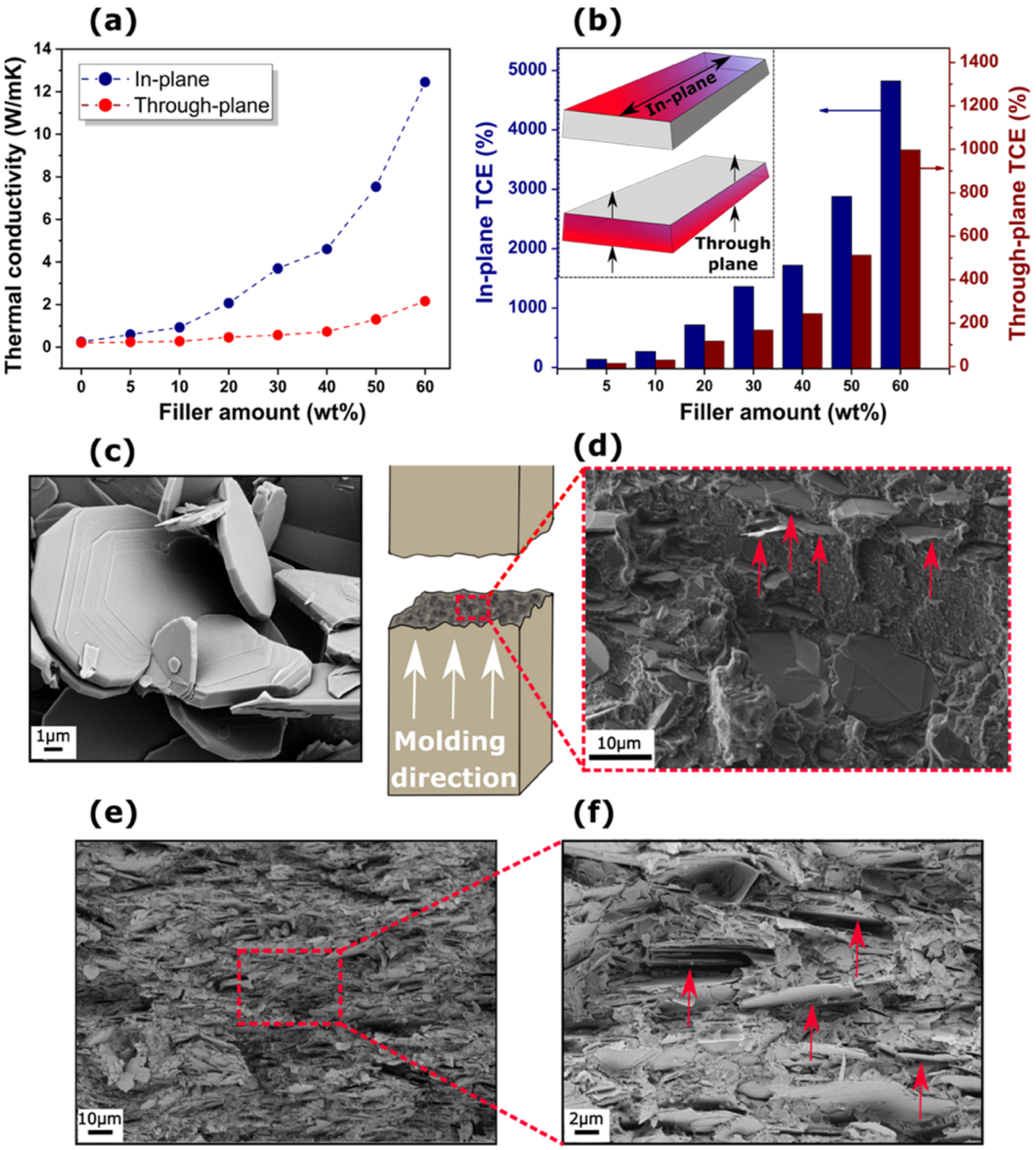

Figure 3. (a) Variation of in-plane and through-plane thermal conductivities of composites as a function of filler loading fraction, (b) thermal conductivity enhancement $\left(\mathrm{TCE} = \frac{\mathrm{TC}_{\mathrm{composite}} - \mathrm{TC}_{\mathrm{PEEK}}}{\mathrm{TC}_{\mathrm{PEEK}}} \times 100\right)$ as a function of filler loading fraction, SEM micrographs of the (c) platelet-type morphology of h-BN powder showing multiple layers held together by weak van der Waals force, (d) cross-sectional view of the fractured PEEK-hBN-5 sample with preferential in-plane orientation of h-BN along the injection-molding direction (as shown by red arrows), (e) cross-section of the PEEK-hBN-60 specimen and the formation of in-plane and through-thickness contact between h-BN clusters (as shown by red arrows).

3.2. Controlling the Thermal Conductivity of hBN-Reinforced PEEK Composites. Thermal management is crucial for the performance, reliability, and lifetime of electronic devices. For applications such as flexible electronics, electronic packaging, light-emitting diodes, and printed circuit boards, heat dissipation is a critical issue as existing polymeric materials suffer from a very low thermal conductivity (T.C). Addressing this challenge requires the development of polymer-based composites with thermally conductive but electrically insulating fillers. Therefore, in this study, hexagonal boron nitride has been used to tune the in-plane ($\kappa_{\parallel}$) and out-of-plane ($\kappa_{\perp}$) thermal conductivities of the PEEK polymer.

Figure 3a shows the variation of $\kappa_{\parallel}$ and $\kappa_{\perp}$ of PEEK/h-BN composites as a function of the h-BN content. The main factors controlling the thermal conductivity of a polymer composite include the matrix thermal conductivity, the amount of filler, the thermal conductivity of filler, and the filler geometry.[35] Since PEEK is a semicrystalline isotropic material, its primary mechanism for heat transfer occurs *via* phonon transport. However, the characteristic morphology of the PEEK polymer causes phonon scattering, thus affecting the average phonon mean free path, and as a result, the thermal conductivity of the bulk polymer is significantly reduced.[50] It can be seen in Figure 3a that the in-plane and through-plane conductivity of the unfilled injection-molded PEEK polymer is

https://doi.org/10.1021/acsapm.2c01534
ACS Appl. Polym. Mater. 2023, 5, 329−341

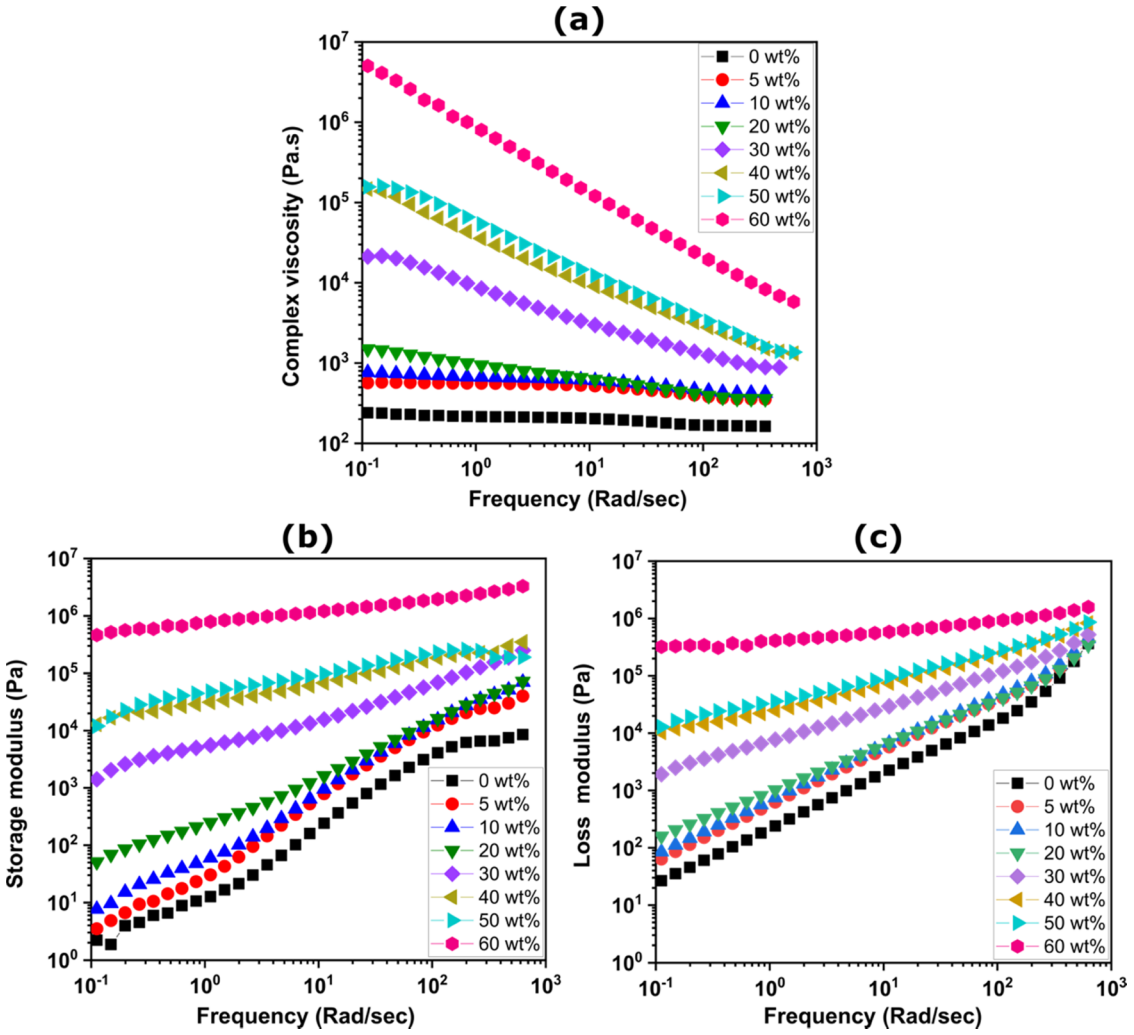

Figure 4. Viscoelastic properties. Variation of (a) complex viscosity, (b) storage modulus, and (c) loss modulus of PEEK/h-BN composites with increase in angular frequency. The provided color-coded legend refers to the concentration (wt %) of h-BN particles in the prepared composites.

0.253 and 0.213 W/mK, respectively. Upon addition of the h-BN filler in the PEEK polymer, T.C in both directions increases. At the highest filler loading, the measured $\kappa_{\parallel}$ and $\kappa_{\perp}$ are 12.451 and 2.337 W/mK, respectively, exceeding that of commercially available thermal interface materials;[51] thus, a thermal conductivity enhancement (TCE%) of 4821% (in-plane) and 997% (through-plane) is achieved. These values have been obtained with a commercial h-BN powder without additional processing steps, so the T.C of PEEK/h-BN composites can be further increased through optimization of filler geometry such as its lateral size and thickness[52] and chain orientation of the PEEK matrix.[53]

Thermal conductivity depends linearly on the loading fraction up to 20 and 40 wt % for $\kappa_{\parallel}$ and $\kappa_{\perp}$ in the composites, respectively. Above these loading fractions, the dependence undergoes a deviation from the linear trend, indicating the onset of the percolation regime.[54,55] Another important observation is that the percolation threshold for in-plane and through-plane conductivity is not achieved at the same filler loading, and the formation of continuous conduction paths through the thickness of composite specimens requires twice as much h-BN fillers compared to the in-plane direction.

The filler shape has a significant influence on the heat conduction of polymer composites. h-BN is a ceramic filler with a high aspect ratio with a platelet-shaped geometry, as shown in Figure 3c. The various layers in a bulk h-BN are held together by weak van der Waals forces, allowing deformation/exfoliation of the stacked layers in the PEEK matrix during processing. For h-BN particles, T.C along the longitudinal direction (~390 W/mK) is much greater than that in the perpendicular direction (~3.3 W/mK).[33] When these platelets are subjected to shear forces during processing, they tend to be aligned parallel to each other and offer a high degree of contact in the parallel direction.[56] Due to this preferential alignment, the manufactured PEEK/h-BN composites show anisotropic behavior since much higher in-plane T.C values are measured compared to $\kappa_{\perp}$ (Table S4).

In the PEEK/h-BN composites, sufficient contact between h-BN platelets in a direction parallel to heat flux is crucial for the formation of thermal pathways to achieve T.C enhancement. At low loadings, the h-BN particles are orientated along the in-plane direction of composites, but the PEEK matrix separates them along the thickness direction. As shown in Figure 3d for the 5 wt % h-BN composite, the contact between the filler clusters is insufficient, and the in-plane and through-plane T.Cs are mainly controlled by the matrix. Since the h-BN particles are isolated and wrapped with the PEEK matrix, the interface thermal resistance between the h-BN particles

https://doi.org/10.1021/acsapm.2c01534
ACS Appl. Polym. Mater. 2023, 5, 329−341

becomes very large, which explains the lowest conductivity improvement in this specimen. The intrinsic out-of-plane T.C of h-BN is low; therefore, to achieve $\kappa_{\perp}$ values of commercial relevance in the PEEK composites, sufficient filler−filler interaction in the thickness direction is crucial. Increasing the filler loading level in current study ensured the formation of efficient thermally conductive pathways through the thickness of specimens, as shown in Figure S2. The measured maximum through-plane T.C reached 2.337 W/mK, superior to those of previously reported h-BN-reinforced thermoplastic composites (Table S5). Figure 3e shows the microstructure of specimen with 60 wt % filler, indicating the presence of percolating networks as the platelets deform during injection-molding to achieve more surface contacts. These results demonstrate that adjusting the loading value for h-BN platelets is a key factor for improving the T.C of the PEEK-based composites, and the greater degree of shear-driven exfoliation during the twin-screw compounding process causes the formation of well-connected filler networks throughout the PEEK polymer.

3.3. Effect of h-BN Loading on the Rheological Performance of PEEK/h-BN Composites. Rheological characterization is an essential tool for conventional and advanced polymer fabrication techniques. The rheological data can be correlated to suitable process parameters for productivity maximization during injection-molding, film fabrication, or additive manufacturing (AM). Extrusion-based deposition processes such as fused filament fabrication (FFF) are the most used AM technologies where a thin filament of a material is melted and then extruded through a nozzle in a defined pattern. 3D printing of high-performance thermoplastics on FFF necessitates structural stability over a wide range of processing conditions, mainly the screw speed and extrusion temperature. Therefore, in the current work, a comprehensive dynamic rheological profile is established through frequency, temperature, and time-dependent rheometry, which can serve as a framework for extrusion-based manufacturing of PEEK/h-BN composites for future studies. The testing temperatures for these measurements were chosen within the bounds defined by the DSC and TGA studies; therefore, the range is kept between the melting point (343 °C) and thermal degradation onset temperature (500 °C) of the composites. After choosing a suitable temperature (Figure S3), dynamic frequency (ω) sweeps are conducted over a range of oscillation frequencies (0.06−628.32 rad/sec) at a constant oscillation amplitude (γ), and the results in terms of complex viscosity (η^*), storage modulus (G'), and loss modulus (G'') are presented in Figure 4. The oscillation amplitude used to determine the dynamic viscoelastic moduli for the neat PEEK and composites up to 30 wt % h-BN was 1%, while that for 40−60 wt % h-BN composites was chosen as 0.1%.

As seen in Figure 4a, the complex viscosity of the composites increases with the addition of h-BN fillers in the whole frequency range. For instance, at ω = 0.1 rad/s, the η^* of specimen with 60 wt % h-BN (4.976 MPa.s) is several orders of magnitude higher compared to the neat PEEK (388.8 Pa.s). As expected, for the neat polymer and composites with low filler content, a Newtonian plateau is observed in the low-frequency range. In contrast, all of the composite specimens demonstrate shear thinning in the high-frequency range. This behavior was also observed for other PEEK composites with flaky fillers as increasing the shear rate results in a breakdown of filler networks.[57] Moreover, on increasing the content of h-BN, the shear-thinning behavior becomes more prominent, presenting a typical characteristic of a non-Newtonian behavior. This property of a composite melt at elevated temperature is critical during FFF as a melt with Newtonian flow or shear-thickening flow can cause printing failure upon application of a higher shear rate by the print-head screw.

The variation of storage (G') and loss moduli (G'') as a function of increasing frequency is presented in Figure 4b,c, respectively. For materials with up to 30 wt % h-BN filler, G'' was found to be higher than the G' by several orders of magnitude across all test frequencies. Adding h-BN fillers to neat PEEK produced composite specimens with greater dynamic moduli compared to the unfilled polymer. When the amount of h-BN in the composite specimen reached 40 wt % and higher, the storage modulus value surpassed the loss modulus. Moreover, at low frequencies (ω < 1 rad/s), the difference in the dynamic moduli of the composite specimens is more significant compared to values observed at high frequencies (ω > 10^2 rad/s), thus suggesting that filler's contribution to the composites' viscoelastic properties in high-frequency ranges is comparatively less pronounced.

If G' > G'', it indicates that the elastic component of the material dominates the viscous components across all frequencies, i.e., viscoelastic solidlike behavior and vice versa. For an extrudate to retain its shape after deposition during extrusion-based 3D printing, it is important to identify which component of the viscoelastic modulus is prevailing. A higher loss modulus (G'' > G') is preferred during injection-molding, where the liquid-dominant behavior of the composite melt is essential, and the mold provides the necessary geometric boundaries. In contrast, for the AM process, a melt with a high loss modulus could result in premature drippage of melt through the nozzle and/or insufficient shape retention of melt bead during printing.[58]

The frequency sweep measurements show that viscosity of the PEEK/h-BN melt is very sensitive to the applied frequency and consequently to the shear strain rate. This information can be useful while selecting process parameters according to the shear rates during an advanced manufacturing process; for instance, powder bed fusion-based processes operate in the very low shear rates (0.002−0.02 s^{-1}),[59] while for extrusion-based 3D printing, the shear rates can be between 100 and 250 s^{-1}[60] .So, by varying the shear rate during the AM process by changing the nozzle geometry, screw profile, and screw speed, the viscosity of the melt can be altered accordingly. Proper viscosity regulation can prevent issues such as filament buckling within nozzle, extrudate swelling, or insufficient layer bonding in the additively manufactured specimens.

PEEK polymers are sensitive to oxidation in the air atmosphere;[61] therefore, it is essential to consider the change in the viscosity of PEEK-based composites, especially if they are to be processed by out-of-autoclave (OOA) manufacturing or 3D printing. The melt viscosity of the PEEK/h-BN composite can be efficiently tuned by changing the temperature. Therefore, as an example, two candidate test temperatures, i.e., 380 °C and 400 °C are chosen to quantify the relationship between viscosity and the allowable residence time of the composite melts. Details of the candidate temperature selection process for time-sweep experiments are provided in Figures S4 and S5.

For generation of the time-sweep results provided in Figure 5a, the composite melts were allowed to reside inside the

https://doi.org/10.1021/acsapm.2c01534
ACS Appl. Polym. Mater. 2023, 5, 329−341

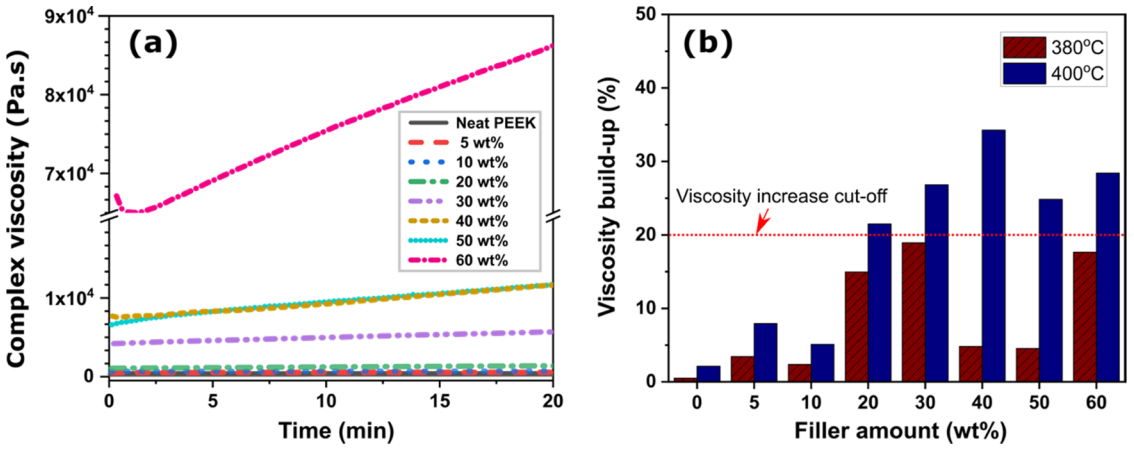

Figure 5. (a) Time evolution of complex viscosity for PEEK/h-BN composites at 380 °C. (b) Viscosity buildup in the PEEK/h-BN composite specimen within 10 min at 380 °C and 400 °C with the dotted line depicting a "safe limit" where viscosity increase is ≤20%.

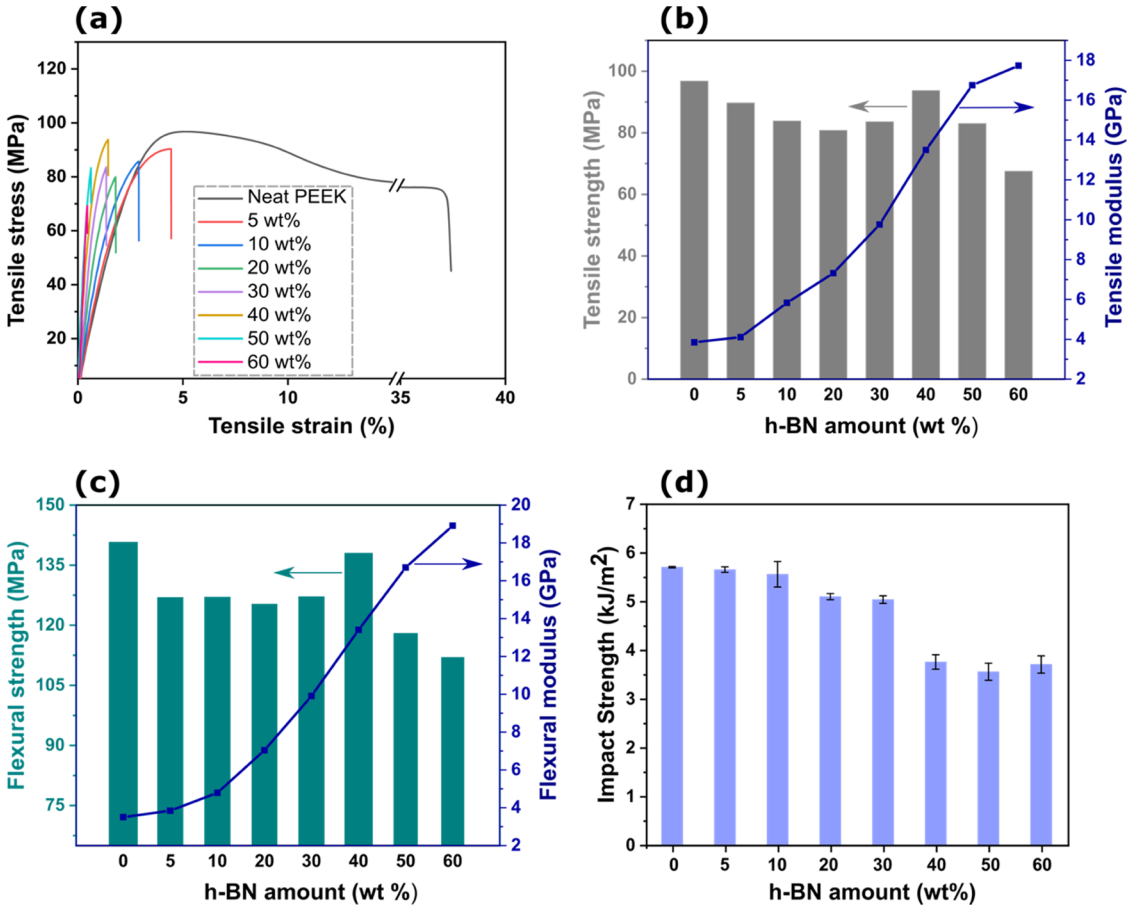

Figure 6. Mechanical properties of PEEK/h-BN composites. (a) Stress vs strain curves during tensile loading, (b) tensile strength and tensile modulus, (c) flexural strength and flexural modulus, and (d) impact strength at 25 °C.

measurement chamber for 20 min at the selected temperature, and the rheological data were collected every 20 s. As expected, for all of the composite specimens, the post condensation of the PEEK matrix facilitated by the heterogeneous nucleation by h-BN particles increases the melt viscosity over time.[59] It can be observed that for neat PEEK, after 20 min, complex viscosity is increased by 1.96%, while under similar conditions, the increase in viscosity at 60 wt % h-BN is as high as 28.29%. These results suggest that increasing the filler amount can reduce the thermal stability of composite melts over longer periods of time, thus significantly altering the viscoelastic properties. For many polymer processing techniques, the residence times are much shorter, i.e., <1 min for powder bed fusion,[59] and <10 min for thermoforming or extrusion-based manufacturing.[62] Therefore, it is critical to investigate the change in viscosity of the material within the time limit established by the chosen composite fabrication method, so that the suitable viscosity−time rheometry profiles can be generated. Like the results provided in Figure 5a, the time-sweep experiments were also conducted at another candidate

https://doi.org/10.1021/acsapm.2c01534
ACS Appl. Polym. Mater. 2023, 5, 329−341

temperature, i.e., 400 °C, and the results are provided in Figure S5. In Figure 5b, the viscosity buildup over a period of 10 min has been plotted for the two candidate temperatures for various PEEK/h-BN composites. The dotted line in Figure 5b represents the viscosity cutoff limit where a change in the complex viscosity is ≤20% to ensure that the material does not lose the beneficial low melt viscosity for easier processing.[62] Based on the structural interactions within the material system, the viscosity buildup within selected time at a particular temperature provides an estimate of the polymer melt stability. At the highest loading of 60 wt %, after a time span of 10 min, the increase in viscosity is 17.64% at 380 °C and 28.51% at 400 °C, suggesting a reduction in melt stability at higher temperature. Such a reduced stability of composite melt could be linked to various factors including reactions at the filler−matrix interface or thermally induced cross-linking of PEEK at a temperature higher than the normal processing temperature.[63,64] In short, to ensure easier processing of specimen with h-BN loading ≥20 wt % at 400 °C, either a short processing cycle can be used or the shear rate can be increased. Thus, the time-sweep rheological studies conclude that unfilled PEEK polymer and composite specimens with a low filler content exhibit superior melt stability at elevated temperatures. Moreover, a shorter residence time is recommended for PEEK/h-BN specimens with a high filler amount to prevent an extreme buildup of viscosity during composite manufacturing.

3.4. Mechanical Properties of the PEEK/h-BN Composites. The mechanical performance of h-BN-reinforced polymeric composites is closely related to efficient load transfer between the matrix and the h-BN particles. To further understand the effect of the microstructure of specimens and filler loading on the mechanical performance of PEEK/h-BN composites, tensile, flexural, and impact tests were performed according to the suitable ISO standards. The tensile stress−strain curves of the composites and pure PEEK are shown in Figure 6a, and the mechanical properties such as tensile strength/modulus, flexural strength/modulus, and impact strength are presented in Figure 6b−d. For the neat PEEK specimen under tensile loading, a typical elastic−plastic deformation can be observed with a tensile strength of 96.87 MPa, tensile modulus of 3.851 GPa, and strain at failure of 23.84%. After adding h-BN particles, the flexural modulus of the fabricated composites is improved significantly, with the highest modulus of 17.73 GPa exhibited at 60 wt % of h-BN, 4.6 times higher than the unfilled PEEK matrix. However, both the tensile strength and strain at break undergo a considerable decrement with increasing the h-BN content. The strain at break decreases from 4.29% for 5 wt % h-BN to 0.47% for 60 wt %, presenting the relatively rigid characteristics of the h-BN particles rather than the PEEK polymer. This is typical behavior of a particulate-reinforced polymer composite, where poor ductility arises due to a weak interface bonding strength between the reinforcing materials and the matrix.

In the current case, as the PEEK polymer is unable to properly wet the filler surface, the formation of continuous phase boundaries is not promoted and the poor interface strength across these phase boundaries directly affects the strength of the composites during mechanical loading. As seen in Table S6, at the highest loading of 60 wt %, a nearly 1/3rd reduction in the tensile strength is observed compared to the unfilled PEEK polymer. The decrease in the tensile strength is usually observed for platelet-filled polymers, and it is due to the pullout of the h-BN platelets owing to insufficient interfacial bonding and the undesired aggregation of h-BN within the matrix. For example, in a study by Wang et al., a 40 wt % boron nitride nanosheet incorporation into a polymer matrix resulted in up to ∼50% tensile strength reduction,[65] likely due to the accumulation of the h-BN sheets within the composites. The contacting points in these agglomerations can either act as crack initiation sites[66] or enhance crack propagation, leading to premature failure of the composites during mechanical loading. Therefore, appropriate surface treatment of h-BN to ensure better wettability in the PEEK matrix can improve the tensile strength of the composites.[19] The incompatibility of the filler surface with the PEEK matrix was captured by XPS characterization, and the results are provided in Figure S6, suggesting the absence of hydroxyl groups on the h-BN surface, which prevents the formation of strong interfacial bonding between the organic PEEK matrix and the inorganic filler. Figure 6c exhibits the flexural strength and modulus of the composite specimens obtained during three-point bending tests. As observed previously in the case of tensile loading, a similar trend is recorded for the flexural properties of the PEEK/h-BN samples as well. Neat PEEK has a flexural strength of 140.75 MPa, flexural modulus of 3.50 GPa, and a failure strain of 6.24% (Table S7). The addition of h-BN particles renders a significant improvement of up to 5.4 times in the flexural modulus of the composites at 60 wt %. However, the poor physical interfacial interactions between h-BN and the polymer matrix resulted in ineffective load transfer and void formation, thus reducing the flexural strength of the composites. For instance, at 5 wt % h-BN, the flexural strength is 126.96 MPa, but it deteriorates rapidly upon increasing the filler amount, reaching the lowest value of 112.00 MPa for PEEK-hBN-60.

In addition to the tensile and flexural testing, the Izod notch impact test was utilized to investigate the impact performance of the prepared PEEK/h-BN composites. The results of the tests in terms of the impact strength of the specimens are provided in Figure 6d. It is readily noticed that the addition of h-BN particles degrades the impact strength of the neat PEEK polymer matrix. As given in Table S8, the lowest impact strength is observed for the composite with 50 wt % of h-BN particles, i.e., 3.56 kJ/m^2, with a 37.56% reduction compared to neat PEEK. The reduction of the impact strength in all of the composite specimens is associated with the increasingly brittle nature of the material as the loading of h-BN increases. As h-BN is not a rubbery filler, the mode of fracture of the composites changes from ductile to brittle,[67] thus reducing the energy absorption during fracture in the composites.[68] In conclusion, the mechanical properties such as tensile modulus and flexural modulus of the PEEK/h-BN composites can be increased significantly by incorporating h-BN particles. However, a decline in ductility and mechanical strength of the composites is recorded compared to the unfilled polymer owing to the insufficient interfacial interactions between the polymer chains and the h-BN particles and the absence of an adequate interface area for stress transfer.

CONCLUSIONS

In the current work, PEEK/h-BN composites with a wide range of h-BN filler content, i.e., 5−60 wt % have been prepared *via* an optimized and scalable co-rotating twin-screw based melt-compounding process. Structural analysis of the prepared composites revealed the high degree of exfoliation

https://doi.org/10.1021/acsapm.2c01534
ACS Appl. Polym. Mater. 2023, 5, 329−341

achieved during processing and the enhanced in-plane alignment of h-BN platelets during injection-molding. Thermal analysis demonstrated that the composites are thermally stable in a wide temperature range with melting and glass transition temperatures comparable to the neat PEEK polymer. Moreover, owing to the nucleation effect of h-BN particles, the specimens possess an accelerated rate of crystallization. Microscopic observations show that h-BN platelets are well dispersed within the PEEK matrix, which led to the formation of continuous heat conduction pathways throughout the specimens. As a result, the measured in-plane and through-plane thermal conductivities at the highest loading were 12.451 and 2.337 W/mK, with an enhancement of 4821% and 997%, respectively, compared to the unfilled PEEK polymer. Rheological characterization of the PEEK/h-BN composites concluded that the melt viscosity of the composites increases with the filler content, and the specimens have a significant shear-thinning behavior in the high-frequency range. Moreover, the time-sweep rheology shows that the viscosity buildup and the allowable residence time during composite manufacturing are strongly linked to the h-BN content and processing temperature, and a shorter residence time is recommended for samples with high filler weight fraction and vice versa to maintain the beneficial low melt viscosity. Mechanical characterization of the PEEK/h-BN composites was performed using tensile, flexural, and Izod impact tests. During tensile and flexural loading, it was found that the higher the h-BN content is, the higher the respective modulus is. However, a degradation of tensile, flexural, and impact strength was observed for the composite specimens compared to neat PEEK, and it is attributed to inadequate interactions and adhesion between the h-BN particles and the matrix. In conclusion, the prepared PEEK/h-BN composites are promising thermal management materials to meet the growing need for heat dissipation in next-generation high-temperature electronics.

■ ASSOCIATED CONTENT

Supporting Information

The Supporting Information is available free of charge at https://pubs.acs.org/doi/10.1021/acsapm.2c01534.

Nomenclature followed for the specimens; XRD parameters of the neat PEEK polymer, bulk h-BN powder, PEEK/h-BN specimens; SEM images of the freeze-fractured PEEK sample and PEEK/h-BN specimens; temperature-dependent rheological characteristics of PEEK/h-BN specimens and time evolution of complex viscosity of the PEEK polymer as a function of time at various temperatures; XPS scan of h-BN powder, thermal parameters of PEEK/h-BN composites; thermal conductivity enhancement and the anisotropy ratio of prepared composites; comparison of thermal conductivity of various BN-filled high-performance thermoplastics; mechanical properties obtained from tensile, flexural, and impact tests of PEEK/h-BN composites (PDF)

■ AUTHOR INFORMATION

Corresponding Author

Burcu Saner Okan − *Sabanci University Integrated Manufacturing Technologies Research and Application Center & Composite Technologies Center of Excellence, Istanbul 34906, Turkey;* orcid.org/0000-0002-5940-7345; Email: burcu.saner@sabanciuniv.edu

Authors

Saher Gul − *Faculty of Engineering and Natural Sciences, Sabanci University, Tuzla, Istanbul 34956, Turkey; Sabanci University Integrated Manufacturing Technologies Research and Application Center & Composite Technologies Center of Excellence, Istanbul 34906, Turkey*

Selin Arican − *Eurotec Engineering Plastics, Avrupa Serbest Bolgesi, Tekirdag 59930, Turkey*

Murat Cansever − *Eurotec Engineering Plastics, Avrupa Serbest Bolgesi, Tekirdag 59930, Turkey*

Bertan Beylergil − *Department of Mechanical Engineering, Alanya Alaaddin Keykubat University, Antalya 07425, Turkey*

Mehmet Yildiz − *Faculty of Engineering and Natural Sciences, Sabanci University, Tuzla, Istanbul 34956, Turkey; Sabanci University Integrated Manufacturing Technologies Research and Application Center & Composite Technologies Center of Excellence, Istanbul 34906, Turkey*

Complete contact information is available at: https://pubs.acs.org/10.1021/acsapm.2c01534

Notes

The authors declare no competing financial interest.

■ ACKNOWLEDGMENTS

Tenmak-Boren, Turkey is kindly acknowledged for providing funding for the current research. Saher Gul kindly acknowledges the financial support provided by Higher Education Commission of Pakistan under the Grant Number 5-1/HRDI-UESTP/359.

■ REFERENCES

(1) He, X.; Wang, Y. Recent Advances in the Rational Design of Thermal Conductive Polymer Composites. *Ind. Eng. Chem. Res.* **2021**, *60*, 1137−1154.

(2) Garimella, S. V.; Fleischer, A. S.; Murthy, J. Y.; Keshavarzi, A.; Prasher, R.; Patel, C.; Bhavnani, S. H.; Venkatasubramanian, R.; Mahajan, R.; Joshi, Y.; Sammakia, B.; Myers, B. A.; Chorosinski, L.; Baelmans, M.; Sathyamurthy, P.; Raad, P. E. Thermal Challenges in Next-Generation Electronic Systems. *IEEE Trans. Comp. Packag. Technol.* **2008**, *31*, 801−815.

(3) Díez-Pascual, A. M.; Naffakh, M.; Marco, C.; Ellis, G.; Gómez-Fatou, M. A. High-Performance Nanocomposites Based on Polyetherketones. *Prog. Mater. Sci.* **2012**, *57*, 1106−1190.

(4) Shukla, D.; Negi, Y. S.; Uppadhyaya, J. S.; Kumar, V. Synthesis and Modification of Poly(Ether Ether Ketone) and Their Properties: A Review. *Polym. Rev.* **2012**, *52*, 189−228.

(5) Cortes, L. Q.; Lonjon, A.; Dantras, E.; Lacabanne, C. High-Performance Thermoplastic Composites Poly(Ether Ketone Ketone)/Silver Nanowires: Morphological, Mechanical and Electrical Properties. *J. Non. Cryst. Solids* **2014**, *391*, 106−111.

(6) Hwang, Y.; Kim, M.; Kim, J. Improvement of the Mechanical Properties and Thermal Conductivity of Poly(Ether-Ether-Ketone) with the Addition of Graphene Oxide-Carbon Nanotube Hybrid Fillers. *Composites, Part A* **2013**, *55*, 195−202.

(7) Liu, L.; Xiao, L.; Zhang, X.; Li, M.; Chang, Y.; Shang, L.; Ao, Y. Improvement of the Thermal Conductivity and Friction Performance of Poly(Ether Ether Ketone)/Carbon Fiber Laminates by Addition of Graphene. *RSC Adv.* **2015**, *5*, 57853−57859.

(8) Díez-Pascual, A. M.; Ashrafi, B.; Naffakh, M.; González-Domínguez, J. M.; Johnston, A.; Simard, B.; Martínez, M. T.; Gómez-Fatou, M. A. Influence of Carbon Nanotubes on the Thermal,

Electrical and Mechanical Properties of Poly(Ether Ether Ketone)/Glass Fiber Laminates. *Carbon* **2011**, *49*, 2817−2833.
(9) Chen, J.; Huang, X.; Sun, B.; Jiang, P. Highly Thermally Conductive Yet Electrically Insulating Polymer/Boron Nitride Nanosheets Nanocomposite Films for Improved Thermal Management Capability. *ACS Nano* **2019**, *13*, 337−345.
(10) Xu, Y.; Chung, D. D. L.; Mroz, C. Thermally Conducting Aluminum Nitride Polymer-Matrix Composites. *Composites, Part A* **2001**, *32*, 1749−1757.
(11) Huang, Y.; Hu, J.; Yao, Y.; Zeng, X.; Sun, J.; Pan, G.; Sun, R.; Xu, J. B.; Wong, C. P. Manipulating Orientation of Silicon Carbide Nanowire in Polymer Composites to Achieve High Thermal Conductivity. *Adv. Mater. Interfaces* **2017**, *4*, No. 1700446.
(12) Yang, N.; Xu, C.; Hou, J.; Yao, Y.; Zhang, Q.; Grami, M. E.; He, L.; Wang, N.; Qu, X. Preparation and Properties of Thermally Conductive Polyimide/Boron Nitride Composites. *RSC Adv.* **2016**, *6*, 18279−18287.
(13) Morishita, T.; Takahashi, N. Highly Thermally Conductive and Electrically Insulating Polymer Nanocomposites with Boron Nitride Nanosheet/Ionic Liquid Complexes. *RSC Adv.* **2017**, *7*, 36450−36459.
(14) Kim, K. K.; Hsu, A.; Jia, X.; Kim, S. M.; Shi, Y.; Dresselhaus, M.; Palacios, T.; Kong, J. Synthesis and Characterization of Hexagonal Boron Nitride Film as a Dielectric Layer for Graphene Devices. *ACS Nano* **2012**, *6*, 8583−8590.
(15) Song, L.; Ci, L.; Lu, H.; Sorokin, P. B.; Jin, C.; Ni, J.; Kvashnin, A. G.; Kvashnin, D. G.; Lou, J.; Yakobson, B. I.; Ajayan, P. M. Large Scale Growth and Characterization of Atomic Hexagonal Boron Nitride Layers. *Nano Lett.* **2010**, *10*, 3209−3215.
(16) Jo, I.; Thompson, M.; Kim, J.; Watanabe, K.; Taniguchi, T.; Yao, Z.; Shi, L. Thermal Conductivity and Phonon Transport in Suspended Few-Layer Hexagonal Boron Nitride. *Nano Lett.* **2013**, *13*, 550−554.
(17) Xie, B. H.; Huang, X.; Zhang, G. J. High Thermal Conductive Polyvinyl Alcohol Composites with Hexagonal Boron Nitride Microplatelets as Fillers. *Compos. Sci. Technol.* **2013**, *85*, 98−103.
(18) Su, K.-H.; Su, C.-Y.; Cho, C.-T.; Lin, C.-H.; Jhou, G.-F.; Chang, C.-C. Development of Thermally Conductive Polyurethane Composite by Low Filler Loading of Spherical BN/PMMA Composite Powder. *Sci. Rep.* **2019**, *9*, No. 14397.
(19) Rasul, M. G.; Kiziltas, A.; Arfaei, B.; Shahbazian-Yassar, R. 2D Boron Nitride Nanosheets for Polymer Composite Materials. *npj 2D Mater. Appl.* **2021**, *5*, No. 56.
(20) Golberg, D.; Bando, Y.; Huang, Y.; Terao, T.; Mitome, M.; Tang, C.; Zhi, C. Boron Nitride Nanotubes and Nanosheets. *ACS Nano* **2010**, *4*, 2979−2993.
(21) Ng, H. Y.; Lu, X.; Lau, S. K. Thermal Conductivity of Boron Nitride-Filled Thermoplastics: Effect of Filler Characteristics and Composite Processing Conditions. *Polym. Compos.* **2005**, *26*, 778−790.
(22) Bujard, P. In *Thermal Conductivity of Boron Nitride Filled Epoxy Resins: Temperature Dependence and Influence of Sample Preparation*, InterSociety Conference on Thermal Phenomena in the Fabrication and Operation of Electronic Components. I-THERM'88; IEEE, 1988; pp 41−49 DOI: 10.1109/itherm.1988.28676.
(23) Zhi, C.; Bando, Y.; Tang, C.; Kuwahara, H.; Golberg, D. Large-Scale Fabrication of Boron Nitride Nanosheets and Their Utilization in Polymeric Composites with Improved Thermal and Mechanical Properties. *Adv. Mater.* **2009**, *21*, 2889−2893.
(24) Teng, C.; Su, L.; Chen, J.; Wang, J. Flexible, Thermally Conductive Layered Composite Films from Massively Exfoliated Boron Nitride Nanosheets. *Composites, Part A* **2019**, *124*, No. 105498.
(25) Xie, S.; Istrate, O. M.; May, P.; Barwich, S.; Bell, A. P.; Khan, U.; Coleman, J. N. Boron Nitride Nanosheets as Barrier Enhancing Fillers in Melt Processed Composites. *Nanoscale* **2015**, *7*, 4443−4450.
(26) Guo, H.; Xu, T.; Zhou, S.; Jiang, F.; Jin, L.; Song, N.; Ding, P. A Technique Engineered for Improving Thermal Conductive Properties of Polyamide-6 Composites via Hydroxylated Boron Nitride Masterbatch-Based Melt Blending. *Composites, Part B* **2021**, *212*, No. 108716.
(27) Zhou, S.; Shi, Y.; Bai, Y.; Liang, M.; Zou, H. Preparation of Thermally Conductive Polycarbonate/Boron Nitride Composites with Balanced Mechanical Properties. *Polym. Compos.* **2020**, *41*, 5418−5427.
(28) Villmow, T.; Kretzschmar, B.; Pötschke, P. Influence of Screw Configuration, Residence Time, and Specific Mechanical Energy in Twin-Screw Extrusion of Polycaprolactone/Multi-Walled Carbon Nanotube Composites. *Compos. Sci. Technol.* **2010**, *70*, 2045−2055.
(29) Müller, M. T.; Krause, B.; Kretzschmar, B.; Pötschke, P. Influence of Feeding Conditions in Twin-Screw Extrusion of PP/MWCNT Composites on Electrical and Mechanical Properties. *Compos. Sci. Technol.* **2011**, *71*, 1535−1542.
(30) Yu, C.; Gong, W.; Zhang, J.; Lv, W.; Tian, W.; Fan, X.; Yao, Y. Hot Pressing-Induced Alignment of Hexagonal Boron Nitride in SEBS Elastomer for Superior Thermally Conductive Composites. *RSC Adv.* **2018**, *8*, 25835−25845.
(31) Wang, X.; Wu, P. Preparation of Highly Thermally Conductive Polymer Composite at Low Filler Content via a Self-Assembly Process between Polystyrene Microspheres and Boron Nitride Nanosheets. *ACS Appl. Mater. Interfaces* **2017**, *9*, 19934−19944.
(32) Liu, X.; Gao, Y.; Shang, Y.; Zhu, X.; Jiang, Z.; Zhou, C.; Han, J.; Zhang, H. Non-Covalent Modification of Boron Nitride Nanoparticle-Reinforced PEEK Composite: Thermally Conductive, Interfacial, and Mechanical Properties. *Polymer* **2020**, *203*, No. 122763.
(33) Yuan, C.; Li, J.; Lindsay, L.; Cherns, D.; Pomeroy, J. W.; Liu, S.; Edgar, J. H.; Kuball, M. Modulating the Thermal Conductivity in Hexagonal Boron Nitride via Controlled Boron Isotope Concentration. *Commun. Phys.* **2019**, *2*, No. 43.
(34) Yu, C.; Zhang, J.; Tian, W.; Fan, X.; Yao, Y. Polymer Composites Based on Hexagonal Boron Nitride and Their Application in Thermally Conductive Composites. *RSC Adv.* **2018**, *8*, 21948−21967.
(35) Chen, H.; Ginzburg, V. V.; Yang, J.; Yang, Y.; Liu, W.; Huang, Y.; Du, L.; Chen, B. Thermal Conductivity of Polymer-Based Composites: Fundamentals and Applications. *Prog. Polym. Sci.* **2016**, *59*, 41−85.
(36) Doumeng, M.; Makhlouf, L.; Berthet, F.; Marsan, O.; Delbé, K.; Denape, J.; Chabert, F. A Comparative Study of the Crystallinity of Polyetheretherketone by Using Density, DSC, XRD, and Raman Spectroscopy Techniques. *Polym. Test.* **2021**, *93*, No. 106878.
(37) Wang, Y.; Chen, B.; Evans, K.; Ghita, O. Enhanced Ductility of PEEK Thin Film with Self-Assembled Fibre-like Crystals. *Sci. Rep.* **2018**, *8*, No. 1314.
(38) Matović, B.; Luković, J.; Nikolić, M.; Babić, B.; Stanković, N.; Jokić, B.; Jelenković, B. Synthesis and Characterization of Nanocrystaline Hexagonal Boron Nitride Powders: XRD and Luminescence Properties. *Ceram. Int.* **2016**, *42*, 16655−16658.
(39) Wang, J.; Ma, F.; Sun, M. Graphene, Hexagonal Boron Nitride, and Their Heterostructures: Properties and Applications. *RSC Adv.* **2017**, *7*, 16801−16822.
(40) Yuan, C.; Duan, B.; Li, L.; Xie, B.; Huang, M.; Luo, X. Thermal Conductivity of Polymer-Based Composites with Magnetic Aligned Hexagonal Boron Nitride Platelets. *ACS Appl. Mater. Interfaces* **2015**, *7*, 13000−13006.
(41) Shen, H.; Guo, J.; Wang, H.; Zhao, N.; Xu, J. Bioinspired Modification of H-BN for High Thermal Conductive Composite Films with Aligned Structure. *ACS Appl. Mater. Interfaces* **2015**, *7*, 5701−5708.
(42) Pan, C.; Kou, K.; Zhang, Y.; Li, Z.; Wu, G. Enhanced Through-Plane Thermal Conductivity of PTFE Composites with Hybrid Fillers of Hexagonal Boron Nitride Platelets and Aluminum Nitride Particles. *Composites, Part B* **2018**, *153*, 1−8.
(43) Ji, C.; Levitas, V. I.; Zhu, H.; Chaudhuri, J.; Marathe, A.; Ma, Y. Shear-Induced Phase Transition of Nanocrystalline Hexagonal Boron Nitride to Wurtzitic Structure at Room Temperature and Lower Pressure. *Proc. Natl. Acad. Sci. U.S.A.* **2012**, *109*, 19108−19112.

(44) Sandler, J.; Werner, P.; Shaffer, M. S. P.; Demchuk, V.; Altstädt, V.; Windle, A. H. Carbon-Nanofibre-Reinforced Poly(Ether Ether Ketone) Composites. *Composites, Part A* **2002**, *33*, 1033−1039.
(45) Blundell, D. J.; Osborn, B. N. The Morphology of Poly(Aryl-Ether-Ether-Ketone). *Polymer* **1983**, *24*, 953−958.
(46) Wu, X.-F.; Zhao, Y.-K.; Li, H.; Zhao, Z.-H.; Sun, Y.; Zhang, H.; Yu, M.-T.; Jia, F.-F. Non-Isothermal Crystallization Kinetics of Polyamide 6/h-Boron Nitride Composites. *J. Macromol. Sci., Part B: Phys.* **2017**, *56*, 170−177.
(47) Ayoob, R.; Alhabill, F.; Andritsch, T.; Vaughan, A. Enhanced Dielectric Properties of Polyethylene/Hexagonal Boron Nitride Nanocomposites. *J. Mater. Sci.* **2018**, *53*, 3427−3442.
(48) Patel, P.; Hull, T. R.; McCabe, R. W.; Flath, D.; Grasmeder, J.; Percy, M. Mechanism of Thermal Decomposition of Poly(Ether Ether Ketone) (PEEK) from a Review of Decomposition Studies. *Polym. Degrad. Stab.* **2010**, *95*, 709−718.
(49) Yu, B.; Xing, W.; Guo, W.; Qiu, S.; Wang, X.; Lo, S.; Hu, Y. Thermal Exfoliation of Hexagonal Boron Nitride for Effective Enhancements on Thermal Stability, Flame Retardancy and Smoke Suppression of Epoxy Resin Nanocomposites via Sol−Gel Process. *J. Mater. Chem. A* **2016**, *4*, 7330−7340.
(50) Mehra, N.; Mu, L.; Ji, T.; Yang, X.; Kong, J.; Gu, J.; Zhu, J. Thermal Transport in Polymeric Materials and across Composite Interfaces. *Appl. Mater. Today* **2018**, *12*, 92−130.
(51) 3M™ Thermally Conductive Silicone Interface Pad 5519 | 3M United States. https://www.3m.com/3M/en_US/p/d/b10134458/ (accessed on September 13, 2021).
(52) Ohashi, M.; Kawakami, S.; Yokogawa, Y.; Lai, G.-C. Spherical Aluminum Nitride Fillers for Heat-Conducting Plastic Packages. *J. Am. Ceram. Soc.* **2005**, *88*, 2615−2618.
(53) Choy, C. L.; Kwok, K. W.; Leung, W. P.; Lau, F. P. Thermal Conductivity of Poly(Ether Ether Ketone) and Its Short-Fiber Composites. *J. Polym. Sci., Part B: Polym. Phys.* **1994**, *32*, 1389−1397.
(54) Kargar, F.; Barani, Z.; Salgado, R.; Debnath, B.; Lewis, J. S.; Aytan, E.; Lake, R. K.; Balandin, A. A. Thermal Percolation Threshold and Thermal Properties of Composites with High Loading of Graphene and Boron Nitride Fillers. *ACS Appl. Mater. Interfaces* **2018**, *10*, 37555−37565.
(55) Bonnet, P.; Sireude, D.; Garnier, B.; Chauvet, O. Thermal Properties and Percolation in Carbon Nanotube-Polymer Composites. *Appl. Phys. Lett.* **2007**, *91*, No. 201910.
(56) Hill, R. F.; Supancic, P. H. Thermal Conductivity of Platelet-Filled Polymer Composites. *J. Am. Ceram. Soc.* **2004**, *85*, 851−857.
(57) Papageorgiou, D. G.; Liu, M.; Li, Z.; Vallés, C.; Young, R. J.; Kinloch, I. A. Hybrid Poly(Ether Ether Ketone) Composites Reinforced with a Combination of Carbon Fibres and Graphene Nanoplatelets. *Compos. Sci. Technol.* **2019**, *175*, 60−68.
(58) Duty, C.; Ajinjeru, C.; Kishore, V.; Compton, B.; Hmeidat, N.; Chen, X.; Liu, P.; Hassen, A. A.; Lindahl, J.; Kunc, V. What Makes a Material Printable? A Viscoelastic Model for Extrusion-Based 3D Printing of Polymers. *J. Manuf. Processes* **2018**, *35*, 526−537.
(59) Yan, M.; Tian, X.; Peng, G.; Li, D.; Zhang, X. High Temperature Rheological Behavior and Sintering Kinetics of CF/PEEK Composites during Selective Laser Sintering. *Compos. Sci. Technol.* **2018**, *165*, 140−147.
(60) Ajinjeru, C.; Kishore, V.; Lindahl, J.; Sudbury, Z.; Hassen, A. A.; Post, B.; Love, L.; Kunc, V.; Duty, C. The Influence of Dynamic Rheological Properties on Carbon Fiber-Reinforced Polyetherimide for Large-Scale Extrusion-Based Additive Manufacturing. *Int. J. Adv. Manuf. Technol.* **2018**, *99*, 411−418.
(61) Pascual, A.; Toma, M.; Tsotra, P.; Grob, M. C. On the Stability of PEEK for Short Processing Cycles at High Temperatures and Oxygen-Containing Atmosphere. *Polym. Degrad. Stab.* **2019**, *165*, 161−169.
(62) Kishore, V.; Ajinjeru, C.; Hassen, A. A.; Lindahl, J.; Kunc, V.; Duty, C. Rheological Behavior of Neat and Carbon Fiber-reinforced Poly(Ether Ketone Ketone) for Extrusion Deposition Additive Manufacturing. *Polym. Eng. Sci.* **2020**, *60*, 1066−1075.
(63) White, K. L.; Jin, L.; Ferrer, N.; Wong, M.; Bremner, T.; Sue, H. J. Rheological and Thermal Behaviors of Commercial Poly-(Aryletherketone)S. *Polym. Eng. Sci.* **2013**, *53*, 651−661.
(64) Phillips, R.; Glauser, T.; Månson, J. A. E. Thermal Stability of PEEK/Carbon Fiber in Air and Its Influence on Consolidation. *Polym. Compos.* **1997**, *18*, 500−508.
(65) Wang, X.-B.; Weng, Q.; Wang, X.; Li, X.; Zhang, J.; Liu, F.; Jiang, X.-F.; Guo, H.; Xu, N.; Golberg, D.; Bando, Y. Biomass-Directed Synthesis of 20 g High-Quality Boron Nitride Nanosheets for Thermoconductive Polymeric Composites. *ACS Nano* **2014**, *8*, 9081−9088.
(66) Zhang, G.; Lu, H.; Mamidwar, S.; Wang, M.Composites. In *Biomaterials Science*; Elsevier, 2020; pp 415−429 DOI: 10.1016/B978-0-12-816137-1.00029-5.
(67) DeArmitt, C.; Hancock, M.Filled Thermoplastics. In *Particulate-FIlled Polymer Composites*; Rothon, R. N., Ed.; RAPRA, 2003; pp 357−424.
(68) Bigg, D. M. Mechanical Properties of Particulate Filled Polymers. *Polym. Compos.* **1987**, *8*, 115−122.